Investigation of Refractory Properties on the Initial Bubble Behavior in the Water Model of Continuous Casting Process

Go-Gi Lee
Dept. MSE, POSTECH, Pohang, Kyungbuk 790-784, South Korea

Seon-Hyo Kim
Dept. MSE, POSTECH, Pohang, Kyungbuk 790-784, South Korea

Brian G. Thomas
Dept. MechSE, UIUC, Urbana, IL 61801, USA

Keywords: Porous refractory, Permeability, Bubble, Nozzle, Continuous casting

Abstract

A water model has been applied to investigate initial bubble behavior using specially-coated samples of porous MgO refractory to simulate the high-contact angle of steel-argon refractory systems with different permeabilities. Air is injected through the porous refractory and travels through many inter-connected pores to exit the surface through “active sites”. An active site is a pore where bubbles exit from the surface of the porous refractory. The effect of refractory properties has been investigated in both stagnant and downward-flowing water. The number of active sites increases with increasing gas injection flow rate, increasing permeability, increasing velocity of the downward-flowing water, and lower contact angle.

Introduction

Argon gas is injected into downward-flowing liquid steel through the Upper Tundish Nozzle (UTN), which connects the tundish bottom and slide gate system. The fluid flow in the Submerged Entry Nozzle (SEN) is highly turbulent, and depends greatly on the amount and size of injected gas. Furthermore, the flow pattern in the mold is greatly affected by the fluid flow at the nozzle ports. Gas bubbles injected through the UTN could penetrate deep into the mold and become entrapped into the solidifying steel shell [1], where they cause blisters and other costly defects [2]. Knowledge and interpretation on the bubble size forming in the nozzle, therefore, is essential for the prediction and understanding of multiphase fluid flow behavior and related defects in the continuous casting process.

Due to the high operating temperature, it is difficult and expensive to directly investigate bubble formation in continuous steel casters [3]. Physical water model experiments with transparent plastic walls, therefore, have been employed to gain insights into single-phase fluid flow in steel casting processes [4-9] where Froude dimensionless number similarity is usually applied, due to the nearly equal kinematic viscosities of molten steel and water. Extensive studies [10-15] of bubble formation were performed on aqueous systems both experimentally and theoretically. Recently, Wang *et al*. [16] used water models to study air-bubble formation from gas injected through a porous refractory into an acrylic nozzle with flowing water. The wettability was reduced by waxing the walls, which caused the gas to form large pockets which travel along the wall and break up into many uneven-sized bubbles. With an unwaxed surface,

relatively uniform-sized bubbles were formed and detached from the wall to join the liquid flow. Although most previous studies are based on bubble formation from an upward-facing orifice or nozzle, some authors [13, 17] observed that bubbles formed from a horizontal orifice behaved almost the same as in stagnant flow. Bai and Thomas [14] developed a correlation to predict average bubble size in both water model experiments and steel–argon systems, as a function of downward water velocity and gas flow rate injected horizontally through drilled holes. However, there is no study on the effect of refractory properties and major processing parameters on bubble formation in the nozzle.

The present study was conducted to quantify bubble size and distribution during gas injection into downward flowing water through realistic porous refractory materials. The effects of liquid velocity, gas flow rate, and contact angle on the mean bubble size, distribution, and the number of active sites on the porous refractory surface will be considered as a parameter to clarify the bubble behavior in a steel caster mold.

Experimental procedure

Figure 1 shows a schematic of the water model apparatus. Water flow in Liter Per Minute (LPM) exits from the tundish bottom through a UTN nozzle. Air is injected through a porous refractory sample (14mm wide x 44mm long x 17mm deep) centered in a representative portion of the nozzle wall. The water flow rate is controlled by the slide gate system to achieve 20 to 45LPM which corresponds to average downward water velocities, V_l, inside the nozzle ranging from 0.68 to 1.58m/s, considering the square 22x22mm nozzle cross-sectional area. The square nozzle shape enables the clear observation of initial bubble behavior inside the nozzle without distortion from refraction.

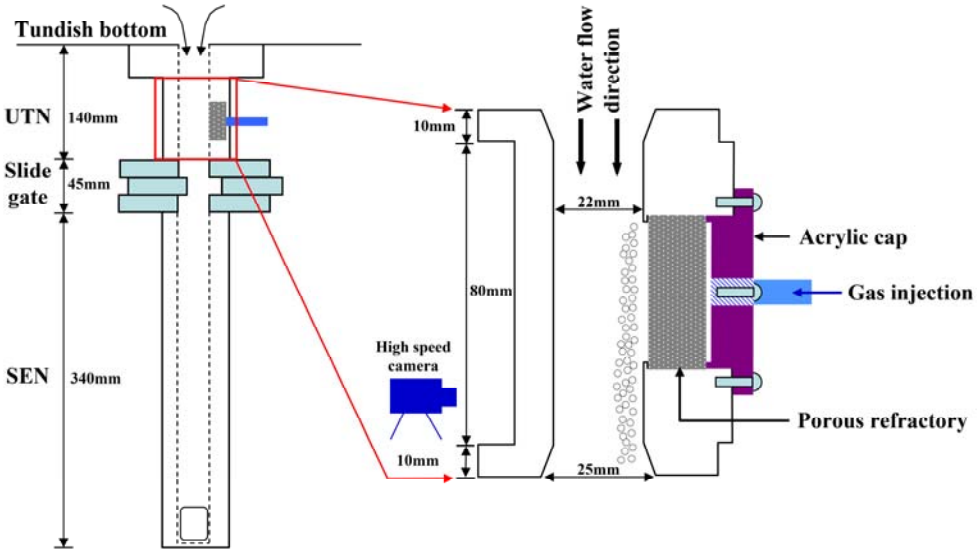

Figure 1 Gas injection through porous MgO refractory UTN

The porous MgO refractory specimens were manufactured with various permeabilities, P_{erm}, as given in Table 1. The wettability between molten steel and the porous refractory has a great influence on bubble formation in the nozzle [18, 19]. To achieve the same poor wettability

(high contact angle) between water and porous refractory simulating the actual system, the surface of the porous MgO refractory was specially treated to lower its wettability. With this method, an active layer was first formed on the surface of porous refractory by oxidizing the surface with O_2 plasma. The refractory is then immersed in Silane solution, (1H,1H,2H,2H Perfluoro-Dodecyltrichlorosilane), which reacts to form a thin siloxane layer (R_2SiO, where R is a hydrogen atom or a hydrocarbon group), as illustrated in Figure 2 [20]. In the adsorption process, the water layer on the MgO attracts the surfactants. The hydrophilic head groups of alkylsilanes (R_nSiX_{4-n}, where X is a hydrolysable leaving group, and R is an alkyl chain or phenyl moiety with an organic functional group) are absorbed gradually onto the water layer. Following the adsorption, the head groups are hydrolyzed into silanols (-nSiOH) and the siloxane bond is finally formed by elimination of H_2O molecules from between silanols. The driving force for self assembly is the *in-situ* formation of polysiloxane, which is connected to a surface silanol group via Si-O-Si bonds.

Table 1 Properties of porous MgO refractory bricks

	Brick 1	Brick 2	Brick 3
Fired B. D. (g/cc)	2.9	2.9	2.8
Porosity (%)	16.2	17.6	17.6
Modulus of rupture (psi)	1085	1119	1467
Average pore perimeter (um)	252	302	306
Average pore area (um^2)	3097	4928	4949
Permeability (nPm)	7.52	16.32	26.12

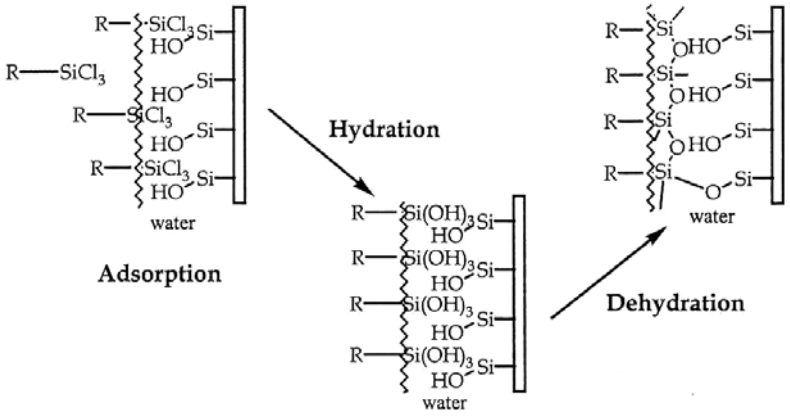

Figure 2 Mechanism of siloxane layer formation [20]

The gas flow rate, Q_g, is adjusted to 0.1 ~ 1.0 Standard Liter Per Minute (SLPM), in order to achieve average injection velocities (flow rates per unit area of refractory surface) of 0.016 ~ 0.162 SLPM/cm^2. The gas is injected into a tube inserted in the back side of the porous refractory specimen, spreads through the many inter-connected pores, and finally leaves the refractory surface. The initial bubble formation before entering slide gate system was recorded by a high speed camera at 4000 frames per second, and then studied by inspecting the video images frame by frame. Representative recorded-images are shown in Figure 3 for three water velocities and gas flow rates. Each pore where bubbles emerge from the porous refractory surface is termed as an “active site”. In addition to counting the active sites, the bubble size and distribution are also

determined by directly measuring the individual video images.

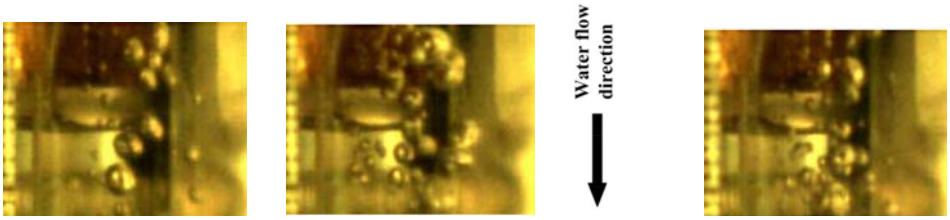

(a) (b) (c)

Figure 3 Photos of water-model experiments with various water velocity V_l and gas velocity V_g in nozzle with 7.52nPm permeability:
(a) V_l =0.97m/s; V_g =0.0027m/s (b) V_l =0.97m/s; V_g =0.0081m/s, and (c) V_l =1.27m/s; V_g =0.0081m/s

Results and discussion

Active site measurement

Water model experiments are first performed in stagnant water by immersing the UTN into a water bath. The results are compared with observations in a nozzle with downward-flowing water at a mean velocity, *U*, of 1.25m/s. For a typical steel casting nozzle of 75mm diameter, (area = 0.00442m^2) this water velocity corresponds with a steel flow rate Q_s of 0.33 m^3/s, or a casting speed V_C of 0.96 m/min for a 230mm x 1500mm slab section, as follows:

$$V_C = \left(\frac{Q_S}{\text{cross-section area of slab}} \right) \tag{3}$$

Figure 4 shows the number of active sites of bubbles evolving from the surface pores of the porous refractory in both stagnant and downward-flowing water systems without surface treatment. Each point for downward-flowing water in Figure 4 represents the mean of five replicate tests performed with identical conditions. The number of active sites consistently increases with increasing gas injection flow rate. Figure 4 clearly shows the effect of downward-flowing velocity increasing the number of active sites, relative to stagnant flow. Drag from the downward-flowing water along the refractory surface acts to shear the bubbles into the water stream before they grow to the mature sizes found in stagnant flow. This drag force produces a smaller bubble size with induced by downward flow, which matches observations by Bai [14]. Fewer active sites form due to the local dynamic pressure drop. The effect of refractory permeability is not clear in downward-flowing water. Whereas, decreasing permeability increases active sites in stagnant flow.

Bubble size and distributions

The water model measurements show that both the mean bubble size and the variation of its distribution increase with increasing gas injection flow rate, and with decreasing water velocity, as shown in Figure 5. Decreasing water velocity below a critical minimum level (such as found in recirculation regions beneath the slide gate) facilitates the formation of very large

bubbles [14]. The periodic release of such large gas pockets might result in significant level fluctuations in the mold, leading to the entrapment of molten mold flux and surface defects associated with an unstable meniscus.

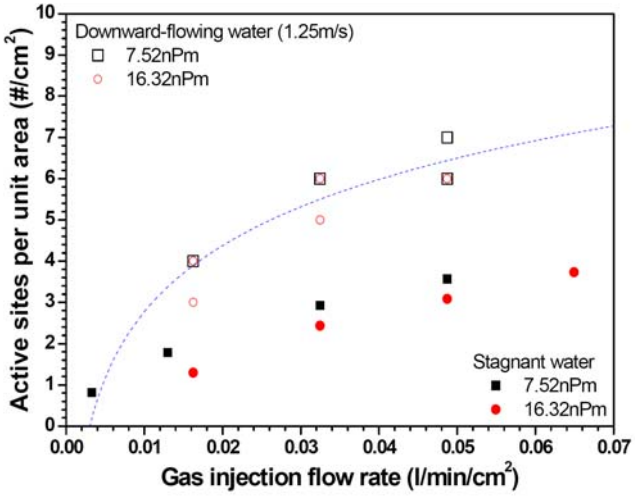

Figure 4 Active sites in both stagnant and downward-flowing water (uncoated refractory)

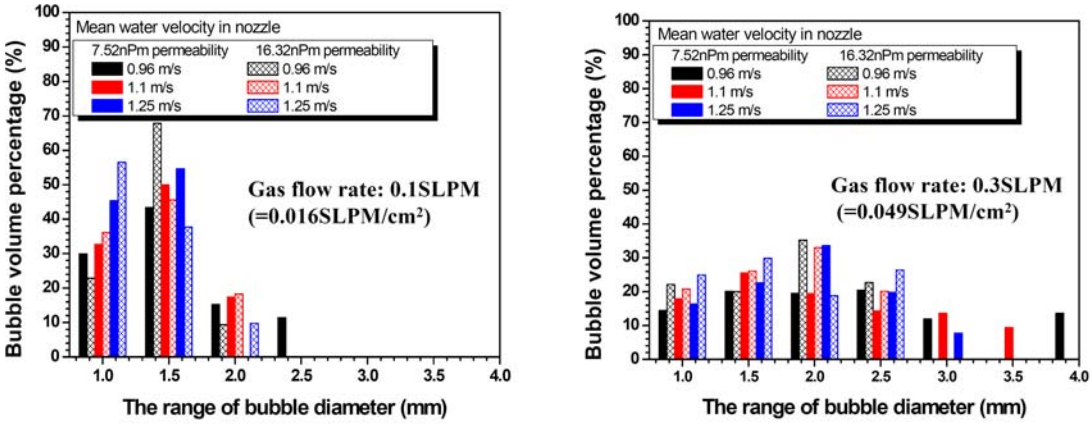

Figure 5 Bubble size distribution with different water velocity and gas flow rate (6.2cm² surface area of uncoated refractory sample)

Effect of wettability on active sites

Figure 6 shows the change of contact angle after coating the surface of porous refractory from 61 deg (uncoated) to ~107 deg (coated). Figure 7 shows the rough surface of the coated refractory using optical microscopy and Scanning Electron Microscope (SEM) for image analysis. The coating layer in Figure 7(b) appears to be ~ 40μm thick, which is smaller than the measured average pore diameter of 80μm. The elements Si and Cl were detected as the main couplers with surface oxygen through Electron Dispersive X-ray Spectroscopy (EDXS). This coating layer is strong enough to persist throughout the water experiments, as evidenced in Figure 7(c).

Figure 8 shows how the number of active sites decreases sharply with higher gas flow

rates after coating the refractory surface. The number of active sites with surface coating decreases, under the same gas flow rate per site, which causes a lower frequency of bubble formation. This finding is consistent with the larger bubble size expected with the low wettability of real molten metal systems. The number of active sites also decreases with decreasing permeability.

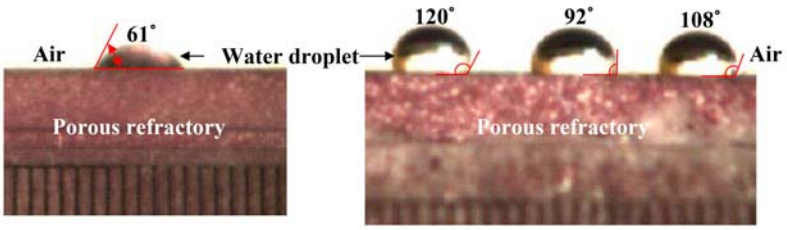

(a) (b)

Figure 6 Contact angle (a) before surface coating, (b) after surface coating

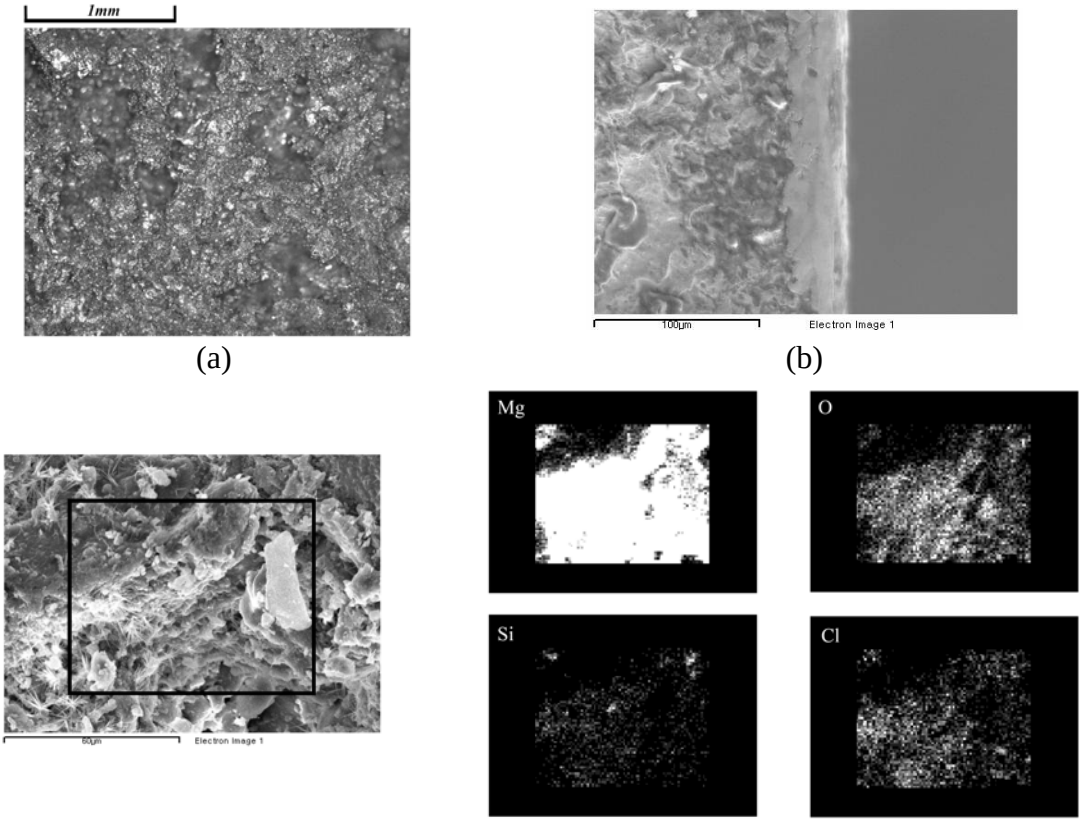

(a) (b)

(c)

Figure 7 Close-up of surface coating with 7.52nPm permeability showing (a) pores (top view), (b) surface coating thickness (side view), and (c) evidence of surface coating material after water experiments

The mean bubble size and its distribution (error bars) with coated refractory was measured as shown in Figure 9. Bubble size is larger with the coated refractory (compare with uncoated in Figure 5). Bubble size of the coated refractory also increases with decreasing permeability and with increasing flow rate, due to the corresponding decrease in number of active sites. Bubble

flow changed from bubbly flow to a continuous gas curtain with gas flow rate increasing above a critical limit of about 0.2 SLPM/cm^2. This makes bubble formation has a much greater tendency to spread into a gas pocket and curtain over the refractory wall. The present work gives new insight into the design of future water models, and also logical investigation of this phenomenon on the initial bubble formation and behavior in the nozzle and mold needs much further work.

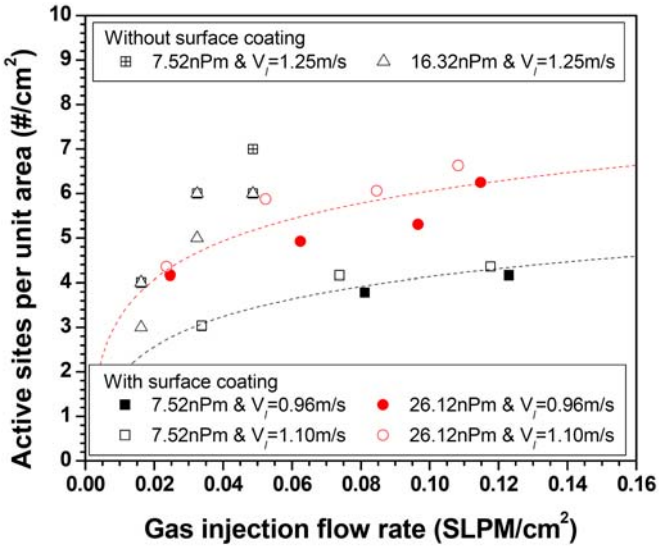

Figure 8 Comparison of active sites with and without surface coating of porous refractory in downward-flowing water

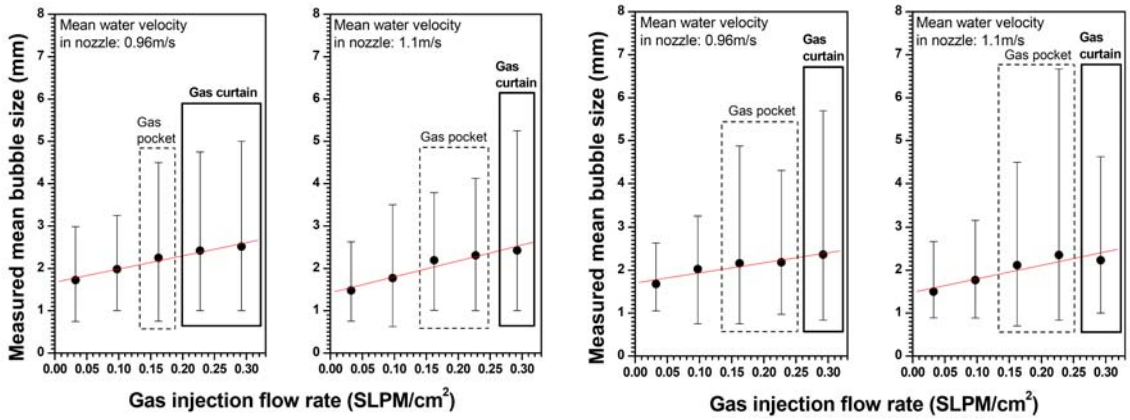

(a) (b)

Figure 9 Bubble size distribution using coated refractory with different permeabilities: (a) 7.52nPm and (b) 26.12nPm

Conclusions

The initial stages of bubble formation injecting gas through porous MgO refractory into a downward turbulent water flow has been studied with water model experiments. The active sites which indicates the actual site exiting bubble on the surface of porous MgO refractory was employed for investigating the effect of refractory properties on bubble formation. The effects of downward-flowing water velocity, gas injection flow rate, and surface contact angle on the

bubble size, distribution, and the active sites were quantified, but further work is needed to investigate initial bubble formation and bubble behavior in the nozzle and mold with higher contact angle. These effects give new insight into multiphase water model experiment to aid in the design of future water models.

Acknowledgements

The authors are grateful to Technology Innovation Center for Metals & Materials at POSTECH for use of their facilities, and also thank to Continuous Casting Consortium at the University of Illinois at Urbana-Champaign for support of this project, especially Rob Nunnington and LWB Refractories for supplying samples.

References

1. Y. Shirota. in *143rd-144th Nishiyama Memorial Seminar*. 1992. Tokyo: ISIJ.
2. J. Herbertson, et al., *Modelling of Metal Delivery to Continuous Casting Moulds*, in *Steelmaking Conf. Proc.* 1991, ISS, Warrendale, PA: Washington, D.C. p. 171-185.
3. B. G. Thomas, et al., *Comparison of four methods to evaluate fluid velocities in a continuous slab casting mold.* ISIJ International, 2001. **41**(10): p. 1262-1271.
4. R. Sobolewski and D.J. Hurtuk, *Water Modeling of Slab Caster Flow Conditions*, in *2nd Process Technology Conf. Proc.* 1982, Iron and Steel Society, Warrendale, PA. p. 160-165.
5. B. G. Thomas, X. Huang, and R.C. Sussman, *Effect of Argon Gas on Fluid Flow in a Continuous Slab Casting Mold.* Metall. Trans. B, 1994. **25B**(4): p. 527-547.
6. D. Gupta and A. K. Lahiri, *A water model study of the flow asymmetry inside a continuous slab casting mold.* Metallurgical and Materials Transactions B-Process Metallurgy and Materials Processing Science, 1996. **27**(5): p. 757-764.
7. D. Gupta, S. Chakraborty, and A.K. Lahiri, *Asymmetry and oscillation of the fluid flow pattern in a continuous casting mould: A water model study.* ISIJ International, 1997. **37**(7): p. 654-658.
8. S. Sivaramakrishnan, B. G. Thomas, and S. P. Vanka, *Large Eddy Simulation of Turbulent Flow in Continuous Casting of Steel*, in *Materials Processing in the Computer Age*, V. Voller and H. Henein, Editors. 2000, TMS, Warrendale, PA. p. 189-198.
9. M. B. Assar, P. H. Dauby, and G.D. Lawson, *Opening the Black Box: PIV and MFC Measurements in a Continuous Caster Mold*, in *Steelmaking Conf. Proc.* 2000, ISS, Warrendale, PA: Pittsburgh, PA. p. 397-411.
10. Tsuge, H., in *Encyclopedia of Fluid Mechnics*, G.P. Co., Editor. 1986: Houston, TX. p. 191-232.
11. N. Rabiger and A. Vogelpohl, in *Encyclopedia of Fluid Mechnics*, G.P. Co., Editor. 1986: Houston, TX. p. 58-88.
12. R. Clift, J. R. Grace, and M. E. Weber, *Bubbles, Drops and Particles*. 1978, New York: Academics Press, INC.
13. R. Kumar and N. R. Kuloor, in *Advances in Chemical Engineering*, A. Press, Editor. 1970: New York. p. 255-368.
14. H. Bai and B.G. Thomas, *Bubble Formation during Horizontal Gas Injection into Downward-Flowing Liquid.* Metallurgical and Materials Transactions B, 2001. **32**(6): p. 1143-1159.
15. L. F. Zhang, et al., *Investigation of fluid flow and steel cleanliness in the continuous*

casting strand. Metallurgical and Materials Transactions B-Process Metallurgy and Materials Processing Science, 2007. **38**(1): p. 63-83.
16. Z. Wang, K. Mukai, and D. Izu, *Influence of wettability on the behavior of argon bubbles and fluid flow inside the nozzle and mold.* ISIJ International, 1999. **39**(2): p. 154-163.
17. G. A. Irons and R. I. L. Guthrie, *Bubble formation at nozzles in pig iron.* Metal. & Material Trans. B., 1978. **9**(2): p. 101-110.
18. Z. Wang, et al., CAMP-ISIJ, 1998. **11**: p. 24.
19. Z. Wang, et al., CAMP-ISIJ, 1997. **10**: p. 68.
20. J. Bryzek, K. Petersen, and W. McCulley, *Micromachines on the march.* IEEE Spectrum, 1994. **31**(5): p. 20-31.